Organometallic Superstructures

DOI: 10.1002/anie.200704450

A Submicrometer Wire-to-Wheel Metamorphism of Hybrid Tridentate Cyclometalated Platinum(II) Complexes**

*Wei Lu, Stephen Sin-Yin Chui, Kwan-Ming Ng, and Chi-Ming Che**

Supramolecular architectures self-assembled from synthetic organic and/or metal–organic molecules are currently of great interest, and aggregates on diverse size scales with widely varying morphologies and functionalities have been obtained in molecular design studies.[1] The incorporation of structural motifs that are responsive to external stimuli (light irradiation or chemical reagents) into organic nanostructures allows subsequent surface modification and morphologic manipulation of these organic superstructures,[2] which include spherical,[3] semispherical,[4] block,[5] fibrillar,[6] sheet,[7] toroidal,[8] and tube[9] shapes self-assembled from metal complexes or metal-containing polymers. Discrete nano- and submicrometer ring-shaped structures may exhibit intriguing physical properties, such as nanoscopic far-infrared optical response and a mesoscopic Aharonov–Bohm effect,[10] due to their unique rotational symmetry. Micrometer-scale toroids have been assembled from a dimeric palladium(II) porphyrin complex through a dewetting process,[8] although submicrometer ring-shaped superstructures assembled from small molecules with high levels of crystallinity remain elusive.

Square-planar platinum(II) complexes have long been known to aggregate in the solid state and in highly concentrated solutions.[11,12] Distinctive anisotropic spectroscopic properties (low-energy absorption and/or emission) have often been observed and cited as a signature for the formation of extended polymeric $Pt^{II}\cdots Pt^{II}$ chains.[12] Recently, several groups have taken advantage of solvophobic $Pt^{II}\cdots Pt^{II}$ interactions to organize discrete molecular platinum(II) complexes into nanowires and microwires that exhibit environment-sensitive emissions and/or semiconducting, liquid-crystalline, or gelating properties.[13] In particular, two platinum(II) complexes containing tridentate cyclometalated ligands, namely the neutral species **1**[14] and the cationic species **2**(PF_6),[13a] have been found to bind to each other to form a hybrid complex (**1**·**2**)(PF_6) [Eq. (a)] which self-

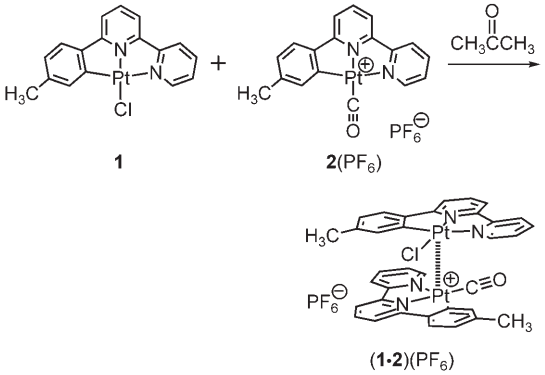

(a)

assembles in concentrated acetone solution into nanowires with diameters of less than 30 nm and lengths of over 30 μm.[13a] These molecular platinum(II) aggregates are quasi-one-dimensional in nature, presumably due to the fact that molecular propagation is faster along the axis of the $Pt^{II}\cdots Pt^{II}$ chain than in the lateral directions.

As the morphology of organic and/or organometallic superstructures can significantly affect their properties, we are presently studying the formation of aggregated platinum(II) complexes at the nano- to micro-scales under various conditions. Herein we report crystalline wheel-shaped superstructures of organoplatinum(II) complexes which grow through a wire-to-wheel metamorphism process involving a ligand-substitution reaction. To the best of our knowledge, this is the first time that organometallic molecules and noncovalent intermolecular metal–metal and ligand–ligand interactions have been used to construct submicrometer-sized nonlinear superstructures. Given the rich optoelectronic properties of organoplatinum(II) complexes,[11e] novel mesoscopic applications based on the superstructures reported herein could be envisaged.

In the present study, we found that the ligand-substitution reaction of the coordinated chloride in **1** with acetonitrile significantly influences the growth of the nanowires derived from (**1**·**2**)(PF_6) when a mixture of acetonitrile and water is used as solvent. The ligand-substitution reaction of **1** with acetonitrile to give $\mathbf{3}^+$ has been reported previously,[15] and complex **3**(PF_6) can be prepared in quantitative yield by refluxing **1** in an acetonitrile/water mixture in the presence of excess NH_4PF_6 [Eq. (b)].[16]

An acetonitrile solution of (**1**·**2**)(PF_6) (6.0×10^{-3} M) was prepared by dissolving equimolar amounts of **1** and **2**(PF_6) in

[*] Dr. W. Lu, Dr. S. S.-Y. Chui, Dr. K.-M. Ng, Prof. Dr. C.-M. Che
Department of Chemistry and HKU-CAS Joint Laboratory on New Materials
The University of Hong Kong
Pokfulam Road, Hong Kong SAR (China)
Fax: (+852) 2857-1586
E-mail: cmche@hku.hk

[**] This work was supported by the Strategic Research Themes on "Bionanotechnology" and "Organic Optoelectronics" of the University Development Fund of The University of Hong Kong, and the Hong Kong Research Grants Council (HKU 7039/03P). W.L. thanks The University of Hong Kong for a University Postdoctoral Fellowship and for a Small Project Funding. We thank Mr. Frankie Yu-Fai Chan and Mr. Wing-Sang Lee of the Electron Microscope Unit of The University of Hong Kong for technical assistance. We also thank the reviewers for their valuable comments.

Supporting information for this article is available on the WWW under http://www.angewandte.org or from the author.

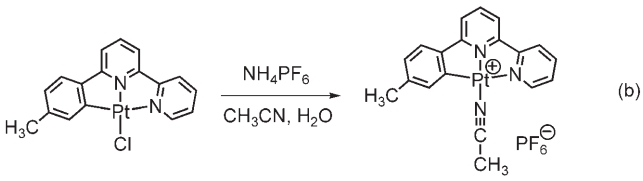

acetonitrile. A 100-μL aliquot of this solution was rapidly added to water (5.0 mL) to give a transparent blue dispersion which shows a distinct low-energy absorption at $\lambda_{max} =$ 604 nm. This characteristic absorption band was attributed to a [dσ*(Pt-Pt)→π*(cyclometalated ligand)] metal-metal-to-ligand charge transfer (MMLCT) transition arising due to the formation of a polymeric $Pt^{II}\cdots Pt^{II}$ chain.[12] A transmission electron microscopy (TEM) image of the initial dispersion showed that it contains nanowires with diameters of around 30 nm and lengths of around 300 nm (see the Supporting Information). This dispersion was either allowed to stand at 25 °C for 48 h (sample A) or isothermalized at 50 °C (sample B) or 70 °C (sample C) for three minutes and subsequently allowed to stand at 25 °C for 48 h. A blue suspension was obtained in all cases. Field-emission scanning electron microscopy (FE-SEM) revealed that these suspensions contain free-standing submicrometer wires and wheels with well-defined facets (Figure 1 a and b for samples A and C, respectively). A few spring-shaped architectures were also found in sample C. Energy dispersion X-ray (EDX) elemental analysis (see the Supporting Information) revealed that the submicrometer wire and wheel structures contain Pt, F, P, and N. The yield of the wheel-shaped superstructures was estimated from the FE-SEM images to be less than 5% for sample A, more than 10% for sample B, and approximately 50% for sample C. Reprecipitation of (**1**·**2**)(PF_6) at a higher temperature (70 °C) in an acetonitrile/water (1:50, v/v) mixture led to the preferential formation of wheel-shaped superstructures.[17]

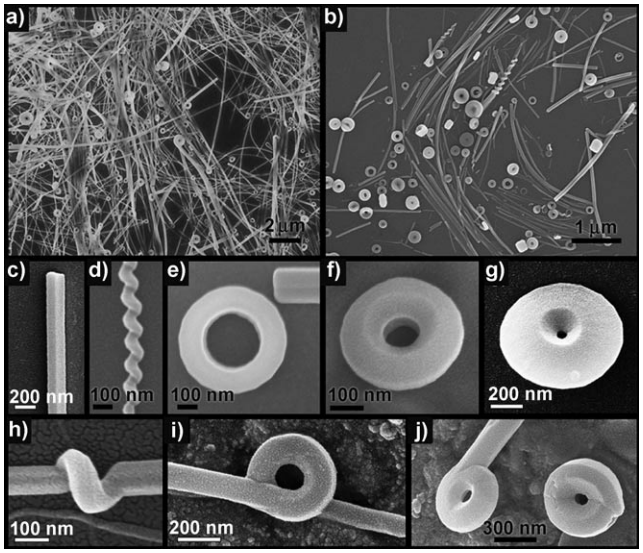

Figure 1. FE-SEM images of the superstructures prepared by precipitating (**1**·**2**)(PF_6) from acetonitrile into water at 25 °C (sample A; a) and at 70 °C (sample C; b). Both dispersions were aged at 25 °C for 24 h. FE-SEM images of freestanding wires (c), springs (d), wheels (e–g), and various intermediate structures (h–j) formed.

Figure 1 c–g show representative FE-SEM images of discrete wires, springs, and wheels. The straight wires are typically around 100 nm high, 100 nm wide, and 3–10 μm long; the cross-sections of these wires are rectangular. The springs are typically 100–150 nm wide, 0.3–1 μm long, and have a pitch of 100–200 nm. Both right- and left-handed helixes can be seen in the FE-SEM images (Figure 1 b). The outer and inner diameters of the wheels vary greatly. Thus, the largest wheels have outer and inner diameters of around 750 and 300 nm respectively, whilst those of the smallest ones are around 100 and 20 nm, respectively. The height (the length of the central channel) of these wheels ranges from 100 to 350 nm. Each discrete wheel consists of 18 equal segments arranged in a circular pattern and the 18 outmost edges and 18 radial grain boundaries can be discerned in the FE-SEM images (amplified images available as Supporting Information). A number of submicrometer superstructures containing joint wire and wheel or wire and spring fragments were also observed in the FE-SEM images (see Figure 1 h–j and the Supporting Information). These superstructures could represent intermediate species that form during the growth process, as discussed below.

To shed light on the structure of the freestanding wheels, it appeared necessary to elucidate the structural characteristics of the microwires. Thus, a crystalline solid sample of (**1**·**2**)-(PF_6) was prepared by reprecipitating equimolar amounts of **1** and **2**(PF_6) from DMF solution (approx. 3×10^{-2} M) into water. A subsequent FE-SEM study revealed that the precipitate contained tabular microwires with a high morphological purity (Figure 2 a). The powder X-ray diffraction (XRD) pattern (Figure 2 b) of a solid sample of (**1**·**2**)(PF_6) containing only microwires was measured and indexed. The low-angle region ($2\theta < 30°$) of the powder XRD data indicated an orthorhombic unit cell with lattice constants $a \approx 25.1$, $b = 9.65$, and $c = 6.70$ Å ($= 3.35$ Å $\times 2$; Figure 2 b, inset). The unusually intense (002) diffraction peak suggests that the nanowires grow preferentially along the c axis (most possibly the long axis of the $Pt^{II}\cdots Pt^{II}$ chains).

The discrete wires and wheels were structurally characterized using data from the TEM and selected area electron diffraction (SAED) patterns (Figure 3). The repeating periods in the SAED pattern of the submicrometer wire (Figure 3 b) were indexed according to the powder XRD data of a crystalline solid sample of (**1**·**2**)(PF_6). The submicrometer wire grows along the [001] direction with a d-spacing of 3.36 Å, which is a typical $Pt^{II}\cdots Pt^{II}$ separation in quasi-one-dimensional cyclometalated platinum(II) or platinum(II) diimine complexes.[11,12] The repeating period of 6.4 Å observed corresponds to the (400) crystal face, which is perpendicular to the wire growth direction (the long axis of the polymeric $Pt^{II}\cdots Pt^{II}$ chain).

Attempts to obtain SAED patterns for the same wheel structure along various other projections were unsuccessful, presumably due to the instability of the organometallic superstructures in the electron beam. The TEM image of a

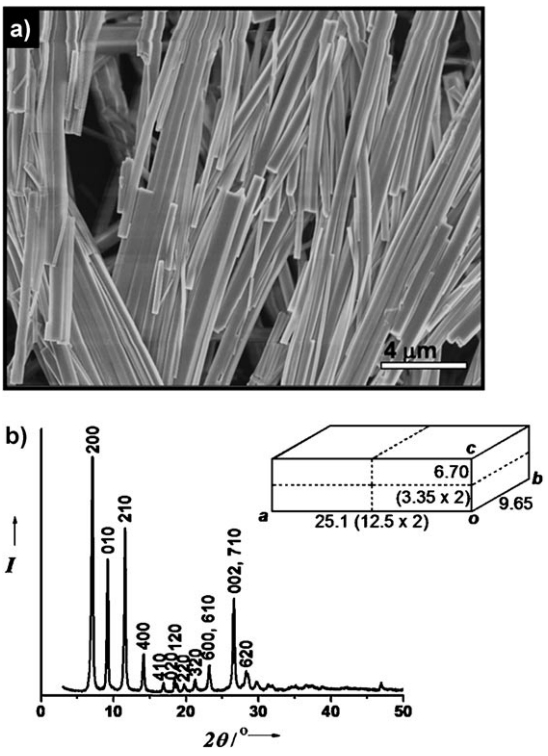

Figure 2. a) FE-SEM image of (**1**·**2**)(PF_6) microwires. b) Powder X-ray diffraction pattern of (**1**·**2**)(PF_6) and the orthorhombic unit cell (inset) deduced from this diffraction pattern.

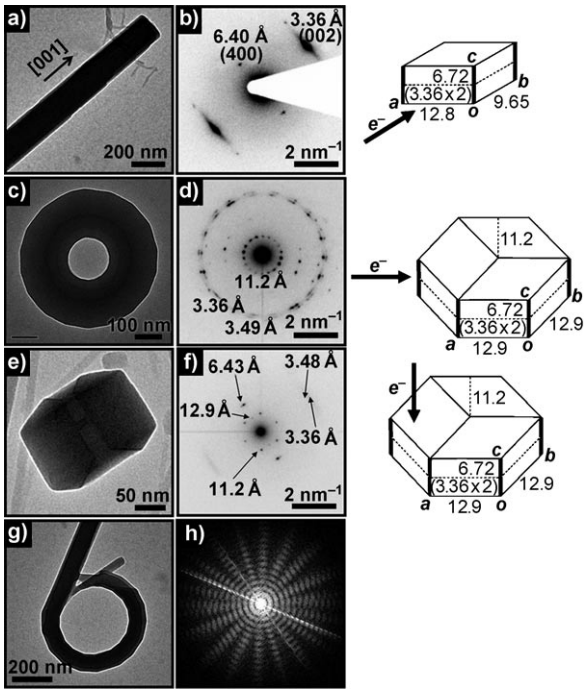

Figure 3. TEM images and the corresponding SAED patterns for submicrometer wires (a and b) and wheels, acquired with an electron beam perpendicular (c and d) and parallel (e and f) to the wheel's basal plane. The TEM images have been rotated by 92° to compensate the image-diffraction pattern rotational angles so that the diffraction pattern coincides in orientation with the respective image. The relationship between the electron diffraction pattern and the electron beam, and the unit cells derived from these electron diffraction data, are shown on the right (errors for lattice parameters are not more than 2%). A TEM image of an intermediate superstructure (g) and its FFT image (h) are also shown.

freestanding wheel (Figure 3c) and its corresponding SAED pattern (Figure 3d) recorded using an electron beam perpendicular to the wheel's basal plane reveal cyclic multiple twins with pseudo-18-fold rotational symmetry and three basic *d* spacings of 3.36, 3.49, and 11.2 Å. The former two *d* spacings are in the same direction and the latter is perpendicular to them. The 18 outmost edges identified from the TEM image are consistent with the SEM observations.

The TEM image of a freestanding wheel (Figure 3e) and its corresponding SAED pattern (Figure 3f) acquired using an electron beam parallel to the wheel's basal plane reveal that there is a repeating period of 11.2 Å with a sixfold rotational symmetry in the sectional plane. There is also a *d* spacing of 12.9 Å along the central channel and two *d* spacings of 3.36 and 3.48 Å perpendicular to the central channel, in other words along the curved circumference of the wheel.

The 2D packing of the polymeric $Pt^{II}\cdots Pt^{II}$ chains is rectangular, with dimensions of 12.8 × 9.65 Å, in the wires and hexagonal, with a side length of 12.9 Å, in the wheels. It should be noted that the cross-sectional dimensions of the wires and wheels are similar to the molecular dimensions of $(\mathbf{1}\cdot\mathbf{2})^+$ (approx. 12 × 8 Å) and $(\mathbf{3}\cdot\mathbf{2})^+$ (approx. 12 × 10 Å; estimations available as Supporting Information). The volume of the unit cell, as calculated from the structural data obtained from the powder XRD, TEM, and SAED studies shown in Figures 2 and 3, increases from 840 $Å^3$ (approx. 12.8 × 9.6 × 6.8) in the wires to 980 $Å^3$ (approx. 12.9 × 11.2 × 6.8) in the wheels. Interestingly, the pseudo-18-fold rotational symmetry could also be identified in the TEM (Figure 3g) and the corresponding fast Fourier transform (FFT; Figure 3h) images of a superstructure containing both wheel and wire fragments. This finding indicates that the symmetry of the wheels develops during the growth process.

We also examined the effect of adding an excess of PF_6^- anions to the superstructures of (**1**·**2**)(PF_6) obtained from an acetonitrile/water dispersion. Thus, a methanolic solution (30 μL, concentration of approximately 0.2 M) of NH_4PF_6 or NH_4Cl (for comparison) was added to a freshly prepared acetonitrile/water (1:50, v/v, 5 mL) dispersion of (**1**·**2**)(PF_6) (concentration: 1.2×10^{-3} M) and the resultant blue suspension stirred at 25 °C for three minutes. The low-energy absorption ($\lambda_{max} = 626$ nm (or 642 nm)) found for the suspension after addition of NH_4PF_6 (or NH_4Cl) is slightly red-shifted with respect to the absorption of the initial dispersion ($\lambda_{max} =$ 604 nm; spectra available as Supporting Information). An FE-SEM image of the (**1**·**2**)(PF_6)/NH_4Cl suspension revealed the presence of entangled nanowires with diameters of around 30 nm (Figure 4a), whereas an FE-SEM image of the (**1**·**2**)(PF_6)/NH_4PF_6 suspension revealed the presence of particles with diameters ranging from 50 to 300 nm (Figure 4b). Dynamic light scattering (DLS) measurements on the particle-size distribution showed that the predominant

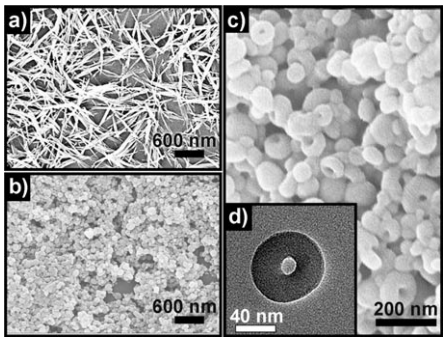

Figure 4. FE-SEM images of the precipitate collected from (**1**·**2**)(PF_6)/NH_4Cl (a) and (**1**·**2**)(PF_6)/NH_4PF_6 suspensions (b and c, at various magnifications). d) TEM image of a discrete nanowheel in the (**1**·**2**)-(PF_6)/NH_4PF_6 suspension.

diameter of the particles within this suspension was around 120 nm. Importantly, the amplified FE-SEM (Figure 4c) and TEM (Figure 4d) images indicated that these particles are nanowheels with inner diameters ranging from a couple of nanometers to as large as 20 nm. No distinct electron diffraction patterns could be recorded for these amorphous nanowheels. Notably, when the concentration of the methanolic NH_4PF_6 solution (30 μL) used was decreased to 0.02 M, both nanowires (major) and nanowheels (minor) were observed in the TEM images of the resultant suspensions (see the Supporting Information), thus indicating an incomplete transformation from nanowires to nanowheels at this lower concentration.[18]

Acetone solutions of the respective superstructures derived from (**1**·**2**)(PF_6) (nanowires, mixture of submicrometer wires and wheels, and nanowheels) were investigated by ESI mass spectrometry (spectra available as Supporting Information). This analysis clearly showed that the submicrometer wheels and nanowheels contain the cation $\mathbf{3}^+$ in addition to **1** and the cation $\mathbf{2}^+$. The ^{1}H NMR spectra of a mixture of submicrometer wires/wheels gave a rough estimation of the molar ratio of $\mathbf{3}^+$ of less than 5%. No ringlike superstructures were observed upon injection of an acetone solution containing equimolar amounts of **2**(PF_6) and **3**(PF_6) (concentration: 1.2×10^{-3} M) or an acetone solution of a mixture of **1**, **2**(PF_6), and **3**(PF_6) in various molar ratios into water.[19] The transformation of **1** into the cation $\mathbf{3}^+$ may occur after the formation of nanowires, and the ringlike superstructures are not likely to self-assemble directly from **1**, **2**(PF_6), and **3**(PF_6) in solution.

The fact that higher reaction temperatures (up to 70 °C) and excess NH_4PF_6 facilitate the formation of ringlike superstructures in aqueous acetonitrile dispersions is in agreement with the reaction of **1** in an acetonitrile/water mixture. The cation $\mathbf{3}^+$ is the thermodynamic product of the chloride/acetonitrile substitution reaction of **1** in an acetonitrile/water solution in the presence of an equimolar quantity of PF_6^- ions. Higher temperatures apparently accelerate the transformation from **1** into $\mathbf{3}^+$. If an excess of NH_4PF_6 is added to the reaction system, the lower solubility of **3**(PF_6) in the acetonitrile/water mixture means that **3**(PF_6) precipitates out of the solution and hence facilitates the transformation from **1** into $\mathbf{3}^+$. It is evident that the acetonitrile solvent and the ligand-substitution reaction (the transformation from **1** into $\mathbf{3}^+$) play a key role in the morphological evolution of the nanoscale aggregates of platinum(II) complexes, therefore we propose a mechanism where the wire-to-wheel metamorphism process is driven by ligand-substitution reactions that are initiated at the surface and possibly extend to the inner chains of the wires[20] (see Scheme 1). The $Pt^{II}\cdots Pt^{II}$ chain is

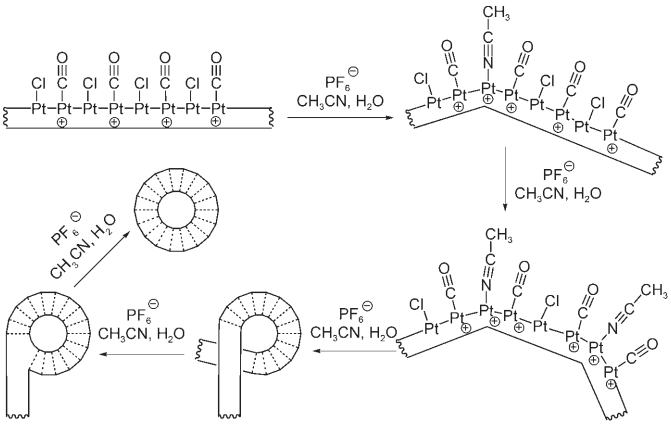

Scheme 1. Diagram illustrating the possible process for the wire-to-wheel metamorphism. The intermediate superstructures drawn are consistent with those found in the FE-SEM images.

perturbed by the electrostatic repulsion between two neighboring cations ($\mathbf{2}^+$ and $\mathbf{3}^+$; $\mathbf{3}^+$ is derived from neutral **1** by the chloride/acetonitrile substitution reaction). These ligand-exchange reactions have two possible consequences: 1) defects are introduced into the $Pt^{II}\cdots Pt^{II}$ chain, which subsequently induces the distortion and bending of the wires, and 2) the 2D packing of the polymeric $Pt^{II}\cdots Pt^{II}$ chains gradually changes from rectangular to hexagonal, and thus the unit cell must expand to accommodate the new acetonitrile ligands. The spring-shaped superstructures may share a similar wire-to-spring growth mechanism. The co-existence of wheels and springs in the reaction mixture is not surprising as these two superstructures are likely to have similar energies. We note that the thinner wires (diameters of less than 100 nm) are more likely to be transformed into springs, presumably due to their lower constraints and higher flexibility.[21]

In summary, we have shown that the subtle interplay between closed-shell $Pt^{II}\cdots Pt^{II}$ interactions and electrostatic/Coulombic interactions leads to the formation of organoplatinum(II) superstructures with diverse morphologies. The preliminary studies carried out have shown that the metamorphism process reported herein can tolerate chemical modification on the cyclometalated ligand; this work will be reported in due course (see the Supporting Information for an example).

Received: September 27, 2007
Revised: March 24, 2008
Published online: May 8, 2008

Keywords: electrostatic interactions · materials science · metal–metal interactions · nanostructures · platinum

[1] a) G. M. Whitesides, J. P. Mathias, C. T. Seto, *Science* **1991**, *254*, 1312 – 1319; b) *Supramolecular Polymers* (Ed.: A. Ciferri), Taylor and Francis, Boca Raton, **2005**.

[2] a) M. Albrecht, M. Lutz, A. L. Spek, G. van Koten, *Nature* **2000**, *406*, 970 – 974; b) W. S. Jin, T. Fukushima, A. Kosaka, M. Niki, N. Ishii, T. Aida, *J. Am. Chem. Soc.* **2005**, *127*, 8284 – 8285; c) J. Motoyanagi, T. Fukushima, N. Ishii, T. Aida, *J. Am. Chem. Soc.* **2006**, *128*, 4220 – 4221; d) A. Ajayaghosh, P. Chithra, R. Varghese, *Angew. Chem.* **2007**, *119*, 234 – 237; *Angew. Chem. Int. Ed.* **2007**, *46*, 230 – 233; e) M. S. Kaucher, W. A. Harrell, Jr., J. T. Davis, *J. Am. Chem. Soc.* **2006**, *128*, 38 – 39; f) R. O. Al-Kaysi, A. M. Müller, C. J. Bardeen, *J. Am. Chem. Soc.* **2006**, *128*, 15938 – 15939; g) S. Kobatake, S. Takami, H. Muto, T. Ishikawa, M. Irie, *Nature* **2007**, *446*, 778 – 781.

[3] a) M. H. Oh, C. A. Mirkin, *Nature* **2005**, *438*, 651 – 654; b) X. P. Sun, S. J. Dong, E. K. Wang, *J. Am. Chem. Soc.* **2005**, *127*, 13102 – 13103; c) Y. J. Li, X. F. Li, Y. L. Li, H. B. Liu, S. Wang, H. Y. Gan, N. Wang, X. R. He, D. B. Zhu, *Angew. Chem.* **2006**, *118*, 3721 – 3725; *Angew. Chem. Int. Ed.* **2006**, *45*, 3639 – 3643.

[4] H. Maeda, M. Hasegawa, T. Hashimoto, T. Kakimoto, S. Nishio, T. Nakanishi, *J. Am. Chem. Soc.* **2006**, *128*, 10024 – 10025.

[5] a) J. A. A. W. Elemans, A. E. Rowan, R. J. M. Nolte, *J. Am. Chem. Soc.* **2002**, *124*, 1532 – 1540; b) S. Vaucher, M. Li, S. Mann, *Angew. Chem.* **2000**, *112*, 1863 – 1866; *Angew. Chem. Int. Ed.* **2000**, *39*, 1793 – 1796.

[6] For selected examples, see: a) M. Enomoto, A. Kishimura, T. Aida, *J. Am. Chem. Soc.* **2001**, *123*, 5608 – 5609; b) L. Valade, H. Casellas, S. Roques, C. Faulmann, D. de Caro, A. Zwick, L. Ariès, *J. Solid State Chem.* **2002**, *168*, 438 – 443; c) J. J. Chiu, C. C. Kei, T. P. Perng, W. S. Wang, *Adv. Mater.* **2003**, *15*, 1361 – 1364.

[7] Z. C. Wang, Z. Y. Li, C. J. Medforth, J. A. Shelnutt, *J. Am. Chem. Soc.* **2007**, *129*, 2440 – 2441.

[8] a) A. P. H. J. Schenning, F. B. G. Benneker, H. P. M. Geurts, X. Y. Liu, R. J. M. Nolte, *J. Am. Chem. Soc.* **1996**, *118*, 8549 – 8552; b) M. C. Lensen, K. Takazawa, J. A. A. W. Elemans, C. R. L. P. N. Jeukens, P. C. M. Christianen, J. C. Maan, A. E. Rowan, R. J. M. Nolte, *Chem. Eur. J.* **2004**, *10*, 831 – 839.

[9] a) X. S. Wang, M. A. Winnik, I. Manners, *Angew. Chem.* **2004**, *116*, 3789 – 3793; *Angew. Chem. Int. Ed.* **2004**, *43*, 3703 – 3707; b) Z. C. Wang, C. J. Medforth, J. A. Shelnutt, *J. Am. Chem. Soc.* **2004**, *126*, 15954 – 15955.

[10] For selected examples, see: a) A. Lorke, R. J. Luyken, A. O. Govorov, J. P. Kotthaus, J. M. Garcia, P. M. Petroff, *Phys. Rev. Lett.* **2000**, *84*, 2223 – 2226; b) M. Grochol, F. Grosse, R. Zimmermann, *Phys. Rev. B* **2006**, *74*, 115416.

[11] a) J. A. Bailey, M. G. Hill, R. E. Marsh, V. M. Miskowski, W. P. Schaefer, H. B. Gray, *Inorg. Chem.* **1995**, *34*, 4591 – 4599; b) C. E. Buss, C. E. Anderson, M. K. Pomije, C. M. Lutz, D. Britton, K. R. Mann, *J. Am. Chem. Soc.* **1998**, *120*, 7783 – 7790; c) S. W. Lai, H. W. Lam, W. Lu, K. K. Cheung, C. M. Che, *Organometallics* **2002**, *21*, 226 – 234; d) V. W. W. Yam, K. M. C. Wong, N. Zhu, *J. Am. Chem. Soc.* **2002**, *124*, 6506 – 6507; e) S. W. Lai, C. M. Che, *Top. Curr. Chem.* **2004**, *241*, 27 – 63.

[12] a) D. M. Roundhill, H. B. Gray, C. M. Che, *Acc. Chem. Res.* **1989**, *22*, 55 – 61; b) V. M. Miskowski, V. H. Houlding, *Inorg. Chem.* **1991**, *30*, 4446 – 4452.

[13] a) W. Lu, V. A. L. Roy, C. M. Che, *Chem. Commun.* **2006**, 3972 – 3974; b) Y. H. Sun, K. Q. Ye, H. Y Zhang, J. H. Zhang, L. Zhao, B. Li, G. D. Yang, B. Yang, Y. Wang, S. W. Lai, C. M. Che, *Angew. Chem.* **2006**, *118*, 5738 – 5741; *Angew. Chem. Int. Ed.* **2006**, *45*, 5610 – 5613; c) F. Camerel, R. Ziessel, B. Donnio, C. Bourgogne, D. Guillon, M. Schmutz, C. Iacovita, J. P. Bucher, *Angew. Chem.* **2007**, *119*, 2713 – 2716; *Angew. Chem. Int. Ed.* **2007**, *46*, 2659 – 2662; d) A. Y. Y. Tam, K. M. C. Wong, G. X. Wang, V. W. W. Yam, *Chem. Commun.* **2007**, 2028 – 2030.

[14] W. Lu, B. X. Mi, M. C. W. Chan, Z. Hui, N. Zhu, S. T. Lee, C. M. Che, *J. Am. Chem. Soc.* **2004**, *126*, 4958 – 4971.

[15] a) E. C. Constable, R. P. G. Henney, T. A. Leese, D. A. Tocher, *J. Chem. Soc. Chem. Commun.* **1990**, 513 – 515; b) E. C. Constable, R. P. G. Henney, T. A. Leese, D. A. Tocher, *J. Chem. Soc. Dalton Trans.* **1990**, 443 – 449.

[16] The single-crystal X-ray diffraction data (see the Supporting Information) showed that **1** and **3**(PF_6) crystallize in monoclinic and orthorhombic systems, respectively. The $\mathbf{3}^+$ cations are stacked into a dimeric structure with a $Pt^{II}\cdots Pt^{II}$ separation of 3.21 Å. Powder X-ray diffraction data indicated that **2**(PF_6) crystallized in a triclinic system.

[17] Submicrometer wires and wheels were both observed in the FE-SEM images of these precipitates when the concentration of the initial acetonitrile solution of **1** and **2**(PF_6) (in a 1:1 molar ratio) was varied from 5.0×10^{-4} to 1.0×10^{-2} M or the acetonitrile/water volume ratio for reprecipitation was increased from 1:100 to 1:10.

[18] For comparison, we also prepared nanowires of (**1**·**2**)(PF_6) in acetone/water, DMF/water, and DMSO/water mixtures (1:50 v/v, 5 mL; (**1**·**2**)(PF_6) concentration of 1.2×10^{-3} M). However, no ringlike superstructures were observed after the addition of a methanolic NH_4PF_6 solution (30 μL; concentration: approx. 0.2 M) to these dispersions.

[19] The total concentration of Pt^{II} ions in these comparison experiments was 2.4×10^{-3} M, the concentration of **1** + **3**(PF_6) was equivalent to that of **2**(PF_6), and the volume ratio of acetone/water was 1:50. The molar ratios of **1**/**2**(PF_6)/**3**(PF_6) investigated were 0.8:1:0.2, 0.6:1:0.4, 0.5:1:0.5, 0.4:1:0.6, and 0.2:1:0.8. All the dispersions were kept at 25 °C for 48 h before observation with an electron microscope.

[20] It has been reported that the reduced volume, and thus the increased surface-to-volume ratio of the nanoparticles, of inorganic nanostructures can be accompanied by a lowering of the phase-transition temperature and an acceleration of ion diffusion from the surface to the inner parts of the nanostructures. See: a) D. H. Son, S. M. Hughes, Y. D. Yin, A. P. Alivisatos, *Science* **2004**, *306*, 1009 – 1012; b) R. D. Robinson, B. Sadtler, D. O. Demchenko, C. K. Erdonmez, L. W. Wang, A. P. Alivisatos, *Science* **2007**, *317*, 355 – 358.

[21] a) E. R. Zubarev, M. U. Pralle, E. D. Sone, S. I. Stupp, *J. Am. Chem. Soc.* **2001**, *123*, 4105 – 4106; b) E. D. Sone, E. R. Zubarev, S. I. Stupp, *Angew. Chem.* **2002**, *114*, 1781 – 1785; *Angew. Chem. Int. Ed.* **2002**, *41*, 1705 – 1709.

